

Al/ α -Sexithiophene /Au Schottky Devices

H. Abd El-Khalek, M. Abd El-Salam and F. M. Amin*

Thin Film Laboratory, Physics Department, Faculty of Science, Suez Canal University, Ismailia, Egypt

Received: 21 Mar. 2019, Revised: 22 May 2019, Accepted: 24 Jun. 2019.

Published online: 1 Jul. 2019.

Abstract: This research work dedicated to studying the dielectric spectroscopy and the conduction mechanism of charge transport of α -sexithiophene (α -6T) thin film. α -6T nanoparticles thin films were synthesized by the thermal evaporation technique. Both X-ray diffraction pattern and transmission electron microscopy show the polycrystalline nature of as-deposited α -6T thin film embedded in the amorphous background with typical nanostructured. The dielectric constant (ϵ'), dielectric loss (ϵ'') and ac conductivity (σ_{ac}) measured as a function of frequency at different temperatures.

The ac conductivity obtained by Jonscher's universal law. The σ_{ac} controlled by both the correlated barrier hopping (CBH) and well-localized hopping model. The increments of frequencies from 0.5 KHz to 20 KHz cause the influence on the values of the ac activation energy, where it decreased from 0.219 eV to 0.070 eV. The value of relaxation time ($\tau_0 = 4.545 \times 10^{-7}$ s) indicated that polarization occurs due to orientational polarization.

Keywords: Nanoparticles; Alpha-Sexithiophene thin film; ac conductivity; Dielectric Properties; Relaxation time.

1 Introduction

Oligothiophenes organic thin films have great attention because of high mobilities, processability, and high chemical stability [1-2]. Conjugated oligomers like α -Sexithiophene (α -6T) is an organic p-type semiconductor. α -6T is a material with high stability, high crystallinity, and high conjugation of π electrons [3-5], so it shows a great performance in electronic and optoelectronic applications such as organic photovoltaics, organic light-emitting diodes, ultrafast spatial modulator, and luminescent diodes [6-11].

Using impedance spectroscopy (IS) is a way to characterize the electrical properties of materials and their interfaces with conducting electrodes [12]. It used to investigate the dynamics of bound or mobile charge in the bulk or interfacial regions of solid or liquid material: ionic, semiconducting, mixed electronic-ionic and even dielectrics [12].

This paper aiming to study the temperature-dependent of dielectric properties such as the dielectric constant (ϵ'), dielectric loss (ϵ'') and ac conductivity (σ_{ac}) of Al/ α -6T/Au device using the conductance G, and capacitance C measurements at the frequency range 42 Hz to 5MHz. The present work deal with measurements at room temperature and above (303-368K).

2 Experimental procedures

The device with sandwich structures of Al/ α -6T /Au fabricated on glass substrates by using a high vacuum Edward-E306A, England coating unit. The thin film of α -6T was fabricated under vacuum at a pressure equal 2×10^{-5} mbar, with growth rate ~ 1 nm/s at room temperature and a film thickness of 100 nm. Both Au and Al electrode deposited at rate ~ 2 nm/s under the pressure of 6×10^{-5} mbar. The active area of the sample was 0.020 cm².

The crystal structure of α -6T for powder and the as-deposited thin film was investigated using an X-ray diffractometer (XRD, Philips model X'pert operated at 40 KV and 30 mA using monochromatic Cu-K α radiation with wavelength $\lambda = 1.54056$ Å) over a 2θ from 5 to 80°. Transmission electron microscope, TEM, JEOL [JEM-2100] was used to investigate morphologies of the α -6T thin film. A computer controlled HIOKI 3531-Hi-tester LCR meter were used to measure the impedance Z, conductance G, and capacitance C in the frequency range 42 Hz to 5MHz, and the temperature range 303-368K.

3. Results and discussions

3.1. Structural characterizations

X-ray diffraction (XRD) diffractogram of α -6T in powder form showed in Fig.1.a which proved the polycrystalline nature of α -6T powder. The estimated values of lattice constants were about $a = 6.03$ (Å) $b = 7.85$ (Å) and $c =$

*Corresponding author e-mail: fatma_m_amin@yahoo.com

44.71(Å) for the monoclinic structure of α -6T [13-14]. Fig. 1.b shows XRD diffractogram of as-deposited α -6T thin film. It was clear that the as-deposited film exhibited a poor crystallinity with a low-intensity diffraction peak at $2\theta=19.91^\circ$.

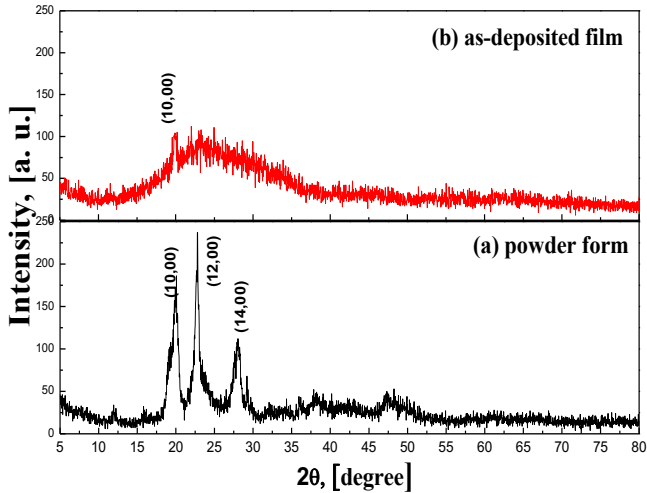


Fig. 1: X-ray diffraction patterns of α -6T in the form of (a) powder and (b) as-deposited thin film

Fig. 2 shows the TEM images and TEM selected-area electron diffraction (SAED) for as-deposited α -6T thin films. Fig. 2 (a- b) indicate that the as-deposited thin film at room temperature (298 K) had a polycrystalline nature in the amorphous background, where the broad-halo at SAED evidence to the existence of an amorphous phase [15]. Also, the spots around halo indicate the polycrystalline nature of film [16].

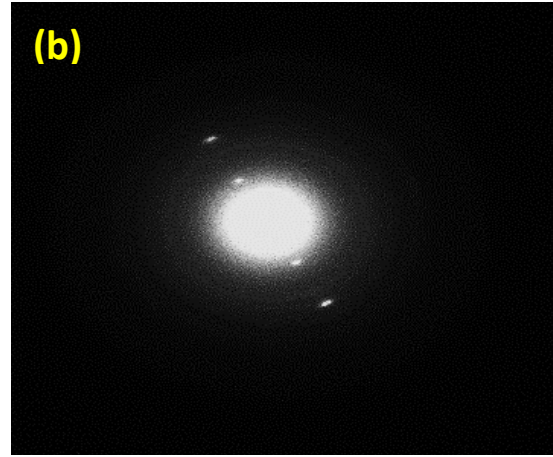
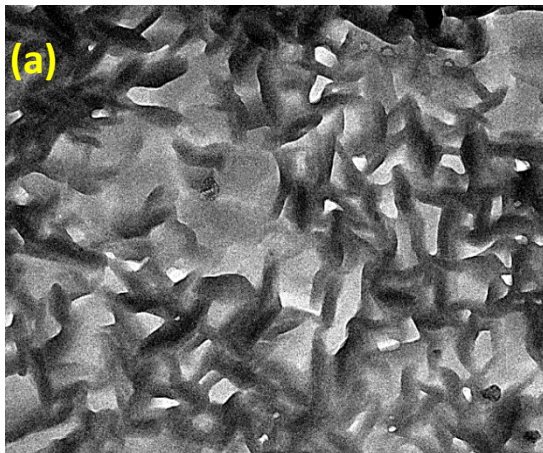


Fig. 2: (a) TEM images and (b) diffraction pattern of α -6T as-deposited thin film

3.2. Dielectric response of alpha-sexithiophene (α -6T) thin film

3.2.1 Dielectric analyses

Dielectric spectroscopy is employed to investigate the charge transport mechanism and relaxation phenomenon in semiconductors. In general, the AC electrical response is a superposition of the dielectric response of the bound charges (dipoles) along with the hopping of the localized charge carriers and the response produced by the molecular structure deformations due to the diffusion of charge carriers [17]. The overall electric behavior can be studied by analyzing various physical quantities, i.e. capacitance, and dielectric permittivity $\epsilon^*(\omega)$ which is particularly useful to study the polarization mechanisms [17].

Dielectric permittivity is expressed as a complex number $\epsilon^*(\omega)=\epsilon'(\omega)-i\epsilon''(\omega)$. The real part of permittivity $\epsilon'(\omega)$ is a measure of how much energy from an external electric field is stored in a material. The imaginary part of permittivity $\epsilon''(\omega)$ is the loss factor and is a measure of how dissipative or lossy a material is to an external electric field. The measurements data of capacitance (C) and conductance (G) were used to calculate both ϵ' and ϵ'' for Al/ α -6T /Au structure (in the temperature range of 303-368K) using the following relations [18-20]:

$$\epsilon' = \frac{C d}{\epsilon_0 A}, \quad (1)$$

$$\epsilon'' = \frac{G}{C_0 \omega}, \quad (2)$$

Where $C_0 = \epsilon_0 A/d$; d is the film thickness, A is the film active area, and ϵ_0 is the permittivity of free space charge. Fig. 3 shows both ϵ' and ϵ'' as a function of frequency at different temperatures.

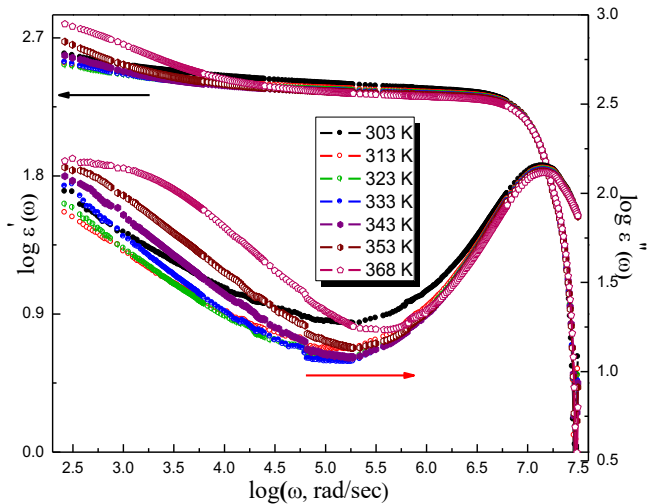


Fig. 3: The frequency dependence of ϵ' and ϵ'' for α -6T film at different temperatures.

The variation in $\epsilon'(\omega)$ values with increasing applied frequency were explained in term of dielectric polarization. This variation passes through three regions. The first region (at low frequencies) where ϵ' decrease as the frequency increase. The second region (at intermediate frequencies) called a saturation region where ϵ' constant. Finally, the third region (at high frequencies) where ϵ' suddenly decrease.

At the low-frequency region, a space charge region at the electrode interface was formed. Interfacial or space charge polarization occurs when the motion of free charges carriers are impeded. Where the charges are captured by various defects within the dielectric without coming into contact with the electrodes. At low frequencies, the charges have time to accumulate at the borders of the conducting regions and produce a dipole moment, which contributes to the polarization causing ϵ' to has large value at low frequency [21-23].

At the intermediate frequency region, the alternating electric field is slow enough that the dipoles are able to keep pace with the field variations. And ϵ' was constant in this frequency region, where $\epsilon' \approx \epsilon_s$ (static dielectric constant) [24]. As the frequency increases, ϵ' begins to decrease due to the phase lag between the dipole alignment and the electric field. Then, ϵ' drops suddenly indicating relaxation process. Above the relaxation frequency both ϵ' and ϵ'' drop off as the electric field is too fast to influence the dipole rotation and the orientational polarization disappears [24]. Fig. 3 also shows the frequency dependence of the imaginary part of the dielectric constant, ϵ'' , for the α -6T thin film at different temperatures. At lower frequencies ϵ'' decreased as the frequency increase, this due to the effect of space charge distribution at the interface between the electrode and α -6T film [21]. A relaxation phenomenon occurs when the excited system returns to its original equilibrium state, this phenomenon appears at higher frequencies [25]. The peaks in the $\epsilon''(\omega)$ indicate a

relaxation process, where the dipoles cannot follow the field variation, so the polarization gradually decreases as ω increases. The loss component in fact represents the dielectric losses in the form of energy absorption. This term is maximum at $\omega_0=1/\tau_0$, where τ_0 is the relaxation time. The value of ω_M determined from the maximum position at the peak which appears in Fig. 3.

The ϵ'' scaled by $\epsilon''_M(\omega)$ and ω scaled by ω_M at different temperatures (303-368 K) as shown in Fig 4. A perfect overlapping of curves for all range of temperatures indicates that the relaxation has the same mechanism over the temperatures range.

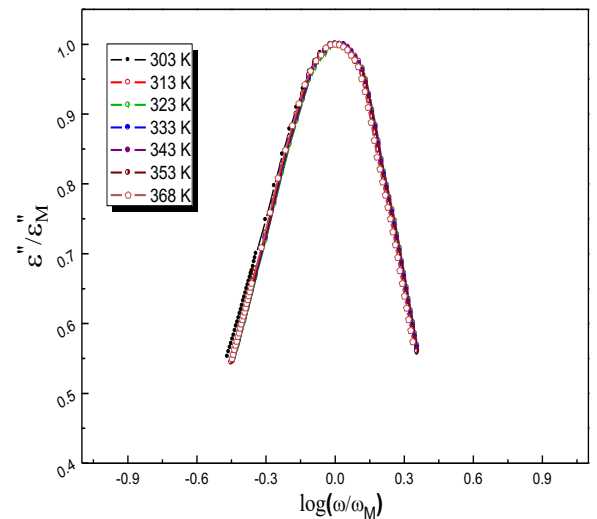


Fig. 4: The scaled imaginary part of dielectric constant ϵ''/ϵ''_M versus $\log \omega/\omega_M$

Using $\omega_0\tau_0 = \omega_{TM} = 1$, the value of τ_0 can be calculated and its value was constant $\sim 4.545 \times 10^{-7}$ (s) as the temperature was increased from 303 to 368 K. The value of τ_0 mean that the polarization occurs due to orientational polarization.

Fig. 5 shows the temperature dependence of the real part of the dielectric constant (ϵ') for an α -6T film at different frequencies. The dielectric constant (ϵ') was increased as the temperature was increased for the frequencies range (0.2-8 KHz). But it decreased as the temperature was increased for the frequencies range (0.06-1 MHz) as shown in the inset of Fig. 5. At low frequencies, the polarization is attributed to space charge (interfacial) polarization, where the space charge polarization is a function of temperature; in most cases, it increases with temperature. So, increase in ϵ' with temperature may be due to the thermal excitation energy which given to charge carriers and made them easily respond to the change in the external field and then enhance the polarization which leads to an increase of the real part of the dielectric constant [23]. At intermediate and high frequencies, the orientational polarization is dominated. At these regions, the thermal

energy tends to randomize the alignment of the permanent dipoles inside the materials. So, ϵ' decreased with increasing temperature [18].

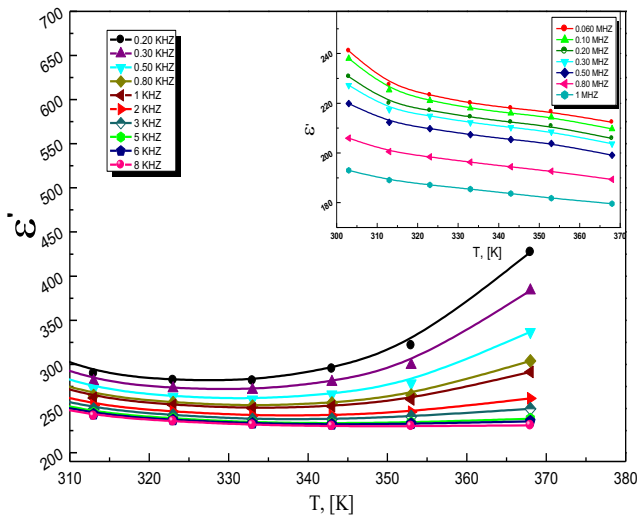


Fig. 5: The temperature dependence of ϵ' for α -6T film at different frequencies

Fig. 6 and the inset in Fig. 6 show the temperature dependence of ϵ'' as a function of frequencies. For the frequencies (0.2-8 KHz) the values of the dielectric loss (ϵ'') increase with the increment of temperature, this due to the increment of σ , and the electrical conduction losses [23]. For high frequencies (0.3-1 MHz) σ decrease and then ϵ'' decrease.

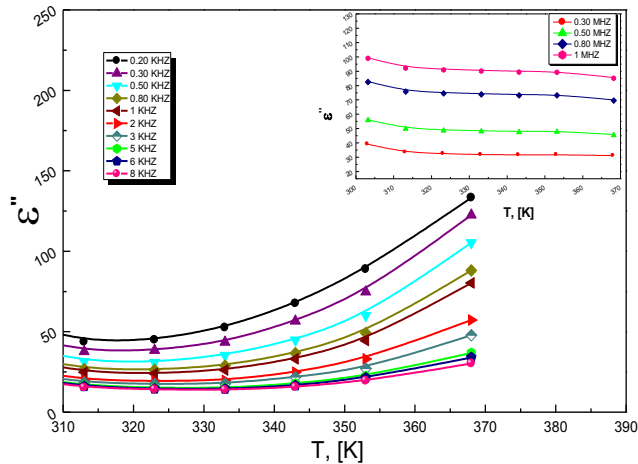


Fig. 6: The temperature dependence of ϵ'' for α -6T film at different frequencies.

3.2.2 Ac conductivity studies

The analysis of AC conductivity is a method to investigate the conduction mechanisms inside the material. The AC conductivity $\sigma_{ac}(\omega)$ for the α -6T thin film is expressed according to Jonscher's law [26-28]:

$$\sigma_{ac}(\omega) = A_1\omega^{s_1} + A_2\omega^{s_2} + A_3\omega^{s_3} \quad (3)$$

where A_1 , A_2 , and A_3 are temperature dependent constants while s_1 , s_2 , and s_3 are frequency and temperature parameters called frequency exponent. Fig. 7 shows the AC conductivity of Al/ α -6T /Au film as a function of frequency and at different temperatures from 303 to 368 K. The value of s in each region was determined by calculating the slope of the linear fitting of each region in Fig. 7.

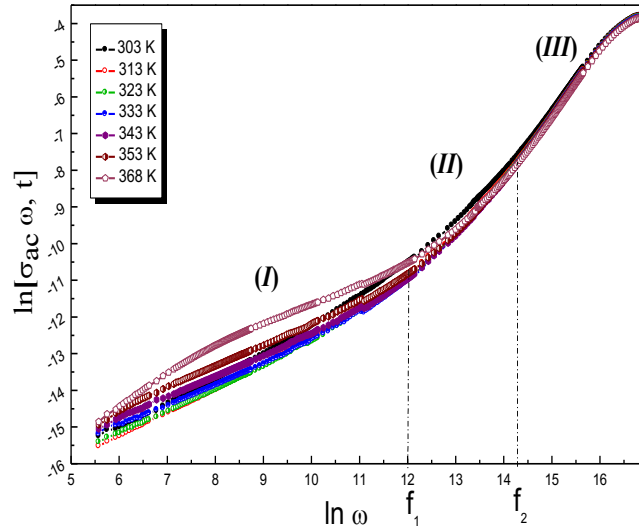


Fig. 7: ac conductivity (σ_{ac}) for α -6T film as a function of frequency at various temperatures.

The behavior of $\ln \sigma_{ac}(\omega)$ with $\ln \omega$ shows three electrical conduction regions: the first one (I) at low frequencies $f < f_1$, the values of s (slope) in this region are less than unity, $0.603 < s < 0.753$, and decreases as temperature increments. In the second (II) and third (III) regions at high frequencies $f > f_1$, the s values in the range $1 < s < 2$. The value of s and its dependence on temperature can define the type of conduction model of α -6T thin film. In the correlated barrier hopping (CBH) model the frequency exponent s is less than unity and is found to decrease with the temperature increment, So The first region in Fig. 7 obeys CBH model [29]. Equation. 4 describe s which related to CBH model [30]

$$s = 1 - \frac{6K_B T}{W_M - K_B T \ln(1/\omega\tau_0)} \quad (4)$$

Where K_B is Boltzmann's constant and W_M is maximum barrier height, at $(\omega_0\tau_0=1)$ the exponent s equal $(s = 1 - \frac{6K_B T}{W_M})$. The W_M take the same trend of s with temperature as shown in Fig. 8.

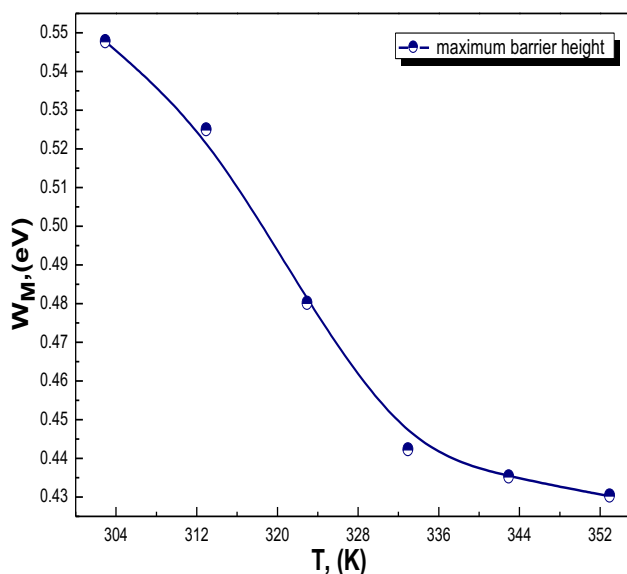


Fig. 8: The maximum barrier height, W_M , dependent on temperature

In the second (II) and third (III) regions, the ac electrical conduction in these regions was due to the well-localized hopping and/or reorientation motion [31].

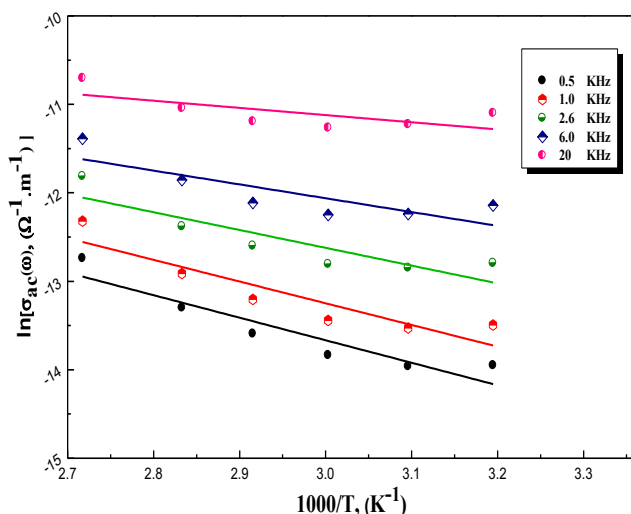


Fig. 9: $\ln \sigma_{ac}$ against $1000/T$ at different frequencies for an α -6T film.

The ac activation energy calculated using Arrhenius' equation (eq. 5) [32]. Fig. 9 shows the plot of $\ln \sigma_{ac}(\omega)$ against $1000/T$.

$$\sigma_{ac}(\omega) = \sigma_o^{\square} \exp \left[-\frac{\Delta E_{ac}}{K_B T} \right], \quad (5)$$

Where σ_o is constant. The increment of frequency from 0.5 to 20 KHz causes the decreases of the activation energy from 0.219 to 0.070 eV. The increment of the applied

frequency enhances the electronic jumps between the localized states [33]. Consequently, the activation energy decrease.

5 Conclusions

α -6T nanoparticles thin films were synthesized by the thermal evaporation technique. Both XRD and TEM show the polycrystalline nature of as-deposited α -6T thin film embedded in the amorphous background with typical nanostructured. The values of both dielectric constant (ϵ') and dielectric loss (ϵ'') were affected by the temperature increment. The value of relaxation time (τ_o) means that polarization occurs due to orientational polarization. The conduction mechanism in an α -6T thin film described by the correlated barrier-hopping (CBH) model. The increment of the applied frequency enhances the values of ac activation energy, which decreased from 0.219 to 0.070 eV.

Acknowledgments

The authors kindly thank Dr. Ahmed M. Nawar from Suez Canal University for his helpful discussion.

References

- [1] J. Casado, M.C. Ruiz Delgado, V. Hernández, J.T. López Navarrete, S. Hotta, F. Carrique and J.R. Ramos-Barrado, *Journal of Non-Crystalline Solids*, 342, 146–151 (2004).
- [2] J. Chisaka, M. Lu, S. Nagamatsu, M. Chikamatsu, Y. Yoshida, M. Goto, R. Azumi, M. Yamashita and K. Yase, *Chemistry of Materials*, 19, 2694–2701 (2007).
- [3] C. Lorch, R. Banerjee, C. Frank, J. Dieterle, A. Hinderhofer, A. Gerlach and F. Schreiber, *The Journal of Physical Chemistry*, 119, 819–825 (2015).
- [4] D. Fichou, *Journal of Materials Chemistry*, 10, 571–588 (2000).
- [5] H. S. Mangold, T. V. Richter, S. Link, U. Würfel and S. Ludwigs, *The Journal of Physical Chemistry. B*, 116, 154–159 (2012).
- [6] T. Mizokuro, K. Takeuchi, C. Heck, H. Aota and N. Tanigaki, *Organic Electronics*, 13, 3130–3137 (2012).
- [7] J. Sakai, T. Taima and K. Saito, *Organic Electronics*, 9, 582–590 (2008).
- [8] C. Heck, T. Mizokuro, M. Misaki, R. Azumi and N. Tanigaki, *Japanese Journal of Applied Physics*, 50, 04DK20 (2011).
- [9] C. Heck, T. Mizokuro and N. Tanigaki, *Applied Physics Express*, 5, 022–103 (2012).
- [10] M. Muccini, *Materials Science and Engineering C*, 5, 173–177 (1998).
- [11] G. Horowitz, P. Delannoy, H. Bouchriha, F. Deloffre, J.L. Fave, F. Gamier, R. Hajlaoui, M. Heyman, F. Kouki, P. Valat, V. Wintgens and A. Yassar, *Advanced Materials*, 6, 752–755 (1994).

- [12] E. Barsoukov and J. R. Macdonald, John Wiley & Sons, Inc (2005).
- [13] S. Nagamatsu, K. Kaneto, R. Azumi, M. Matsumoto, Y. Yoshida and K. Yase, *The Journal of Physical Chemistry*, 109, 9374-9378 (2005).
- [14] S. Ikeda, M. Kiguchi, Y. Yoshida, K. Yase, T. Mitsunaga, K. Inaba and K. Saiki, *Journal of Crystal Growth*, 265, 296–301 (2004).
- [15] M. Ohring, *materials science of thin films*, Academic Press, (2001).
- [16] A.S. Pugalenthi, R. Balasundaraprabhu, S. Prasanna, S. Habibuddin, N. Muthukumarasamy, G. Mohan Rao and M.D. Kannan, *Optical Materials*, 62, 132-138 (2016).
- [17] J. Trzmiel, A. Sieradzki, A. Jurlewicz and Z.T. Kuznicki, *Current Applied Physics*, 14, 991-997(2014).
- [18] A. Karabulut, A. Türüt and Ş. Karataş, *Journal of Molecular Structure*, 1157, 513-518 (2018).
- [19] A. Tataroğlu, İ. Yücedağ and Ş. Altındal, *Microelectronic Engineering*, 85, 1518–1523 (2008).
- [20] Sh.M. Morgan, N.A. El-Ghamaz and M.A. Diab, *Journal of Molecular Structure*, 1160, 227-241(2018).
- [21] D. Arun Kumar, S. Selvasekarapandian, H. Nithya, A. Sakunthala and M. Hema, *Physica B*, 405, 3803–3807 (2010).
- [22] P. Kumar, B.P.Singh, T.P.Sinha and N.K.Singh, *Physica B*, 406, 139–143 (2011).
- [23] E.M. El-Menyawy, H.M. Zeyada and M.M. El-Nahass, *Solid State Sciences*, 12, 2182-2187 (2010).
- [24] D. K Mahato, A. Dutta and T. P. Sinha, *Bulletin of Materials Science*, 34, 455–462 (2011).
- [25] K. C. Kao, *Dielectric Phenomena in solids*, Elsevier Academic Press, (2004).
- [26] I. Khorchani, O. Hafef, J. Reinoso, A. Matoussi, and J.F. Fernandez, *Materials Chemistry and Physics*, 212, 187-195 (2018).
- [27] S. R. Elliott, *Advances in Physics*, 36, 135-218 (1987).
- [28] A. El-ghandour, N.A. El-Ghamaz, M.M. El-Nahass and H.M. Zeyada, *Physica E: Low-dimensional Systems and Nanostructures*, 105, 13–18 (2019).
- [29] I. Bechibani, A. Zaafouri, M. Dammak and L. Ktari, *Journal of Alloys and Compounds*, 724, 951-958 (2017).
- [30] A.A.M. Farag, A.M. Mansour, A.H. Ammar, M. Abdel Rafea and A.M. Farid, *Journal of Alloys and Compounds*, 513, 404– 413 (2012).
- [31] A. Saif and P. Poopalan, *Journal of Materials Science & Technology*, 27, 802-808 (2011).
- [32] A.A. Atta, *Journal of Alloys and Compounds*, 480, 564–567(2009).
- [33] A.A.M. Farag, F.S. Terra and G.M. Mahmoud, *Synthetic Metals*, 160, 743–749 (2010).